Supporting Information
Regulating Ni^{3+} contents by Cobalt doping strategy in ternary $Ni_xCo_{3-x}Al_1$-LDH nanoflowers for high-performance charge storage

Jiaqi Zhang[1], Ningqiang Sun[1], Baoyi Yin[2], Su Yuanhui[1], Shuaijing Ji[1], Yu Huan[1]*, Tao Wei[1]*

[1] School of Materials Science and Engineering, University of Jinan, Jinan 250022, China.

[2] School of Microelectronics, Dalian University of Technology, Dalian, 116024, China.

* Correspondence: mse_huany@ujn.edu.cn (Y. Huan.), mse_weit@ujn.edu.cn (T. Wei).

1. Reagents.

All nitrates and KOH used in the experiment were purchased from Sinopharm Chemical Reagent Co., Ltd. Ammonium fluoride was purchased from Shanghai Macklin Biochemical Co., Ltd, Urea was purchased from Damao Chemical Reagent Factory, ammonium fluoride was purchased from Shanghai McLean Biochemical Co.,Ltd. Polyvinylidene fluoride and conductive carbon black were purchased from Guangdong Canrd New Energy Technology Co.,Ltd. Active carbon materials were purchased from Nanjing Xianfeng Nanomaterial Technology Co., Ltd.,all reagents do not need to be purified.

2. Characterization.

A scanning electron microscopy (SEM; Leo-1530, Oberkochen, Germany) was used to characterize the morphologies and EDS mappings of $Ni_xCo_{3-x}Al_1$-LDH nanoflowers. The structural characteristics of the samples were tested by X-ray diffraction (XRD) in a 2θ range from 10 to 90° (D8 Advance, Bruker, Germany). X-ray photoelectron spectroscopy (XPS, Thermo Fisher Scientific ESCALAB Xi^+) analyses were carried out for the characterization of elemental composition and valence analysis. Transmission electron m icroscopy (TEM), high-resolution transmission electron microscopy (HRTEM) were carried out on electron microscope JEM-2011Plus (JEOL Ltd., Tokyo, Japan) at 200 kV. Fourier transform infrared spectra (FT-IR) of the prepared samples were obtained by using an infrared spectrometer (Nicolet 380,Thermo). The Raman spectra of the materials were measured with a Raman spectrometer (HR Evolution,Horiba). The adsorption-desorption isotherms of the materials were obtained by using kuBO-X1000 specific surface area and pore size analyzer(Beijing Builder Electronic Technology Co., LTD).

3. Electrochemical measurements.

Cyclic voltammetry (CV) was conducted via an electrochemical workstation (CHI600e, Chenhua, Shanghai). Wuhan LANDdt battery test system (Wuhan LAND Electronic Co.Ltd.) was used for constant current charge and discharge test of electrode materials. Electrochemical impedance spectroscopy was tested at the ZAHNER Electrochemical Workstation (IM6, Germany). The electrochemical performances of electrode materials were measured in a three electrode system, which was composed of a counter electrode of Pt, a reference electrode of Ag/AgCl, and an electrolyte of 6 M KOH solution. The preparation of the working electrodes was as

follows: NiCoAl-LDH (80 wt %), carbon black (10 wt %), and PVDF (10 wt%) binder in NMP solution were stirred to acquire uniform slurry, which was subsequently brushed on cleaned carbon paper (1 × 1cm^2) and dried at 60 °C for 12 h. The mass loading of active materials on a single electrode was about 0.8–1.2 mg. The specific capacitance of prepared samples was calculated from GCD curves according to the Eq. (1)

$$C = \frac{I\Delta t}{\Delta m} \tag{1}$$

where *Cs*, *I*, Δt and m represent the specific capacitance (C g^{-1}),discharge current (A), discharge time (s) and weight of the active material in the electrode (g), respectively.

The mass ratio of the positive electrode and negative electrode was calculated by the specific capacitance according to charge balance equation (2):

$$\frac{\mathrm{m}_+}{\mathrm{m}_-} = \frac{C_- \Delta V_-}{C_+ \Delta V_+} \tag{2}$$

where *m*, *C*, and *V* are the mass, specific capacitance, and voltage window of each electrode, respectively.

The specific capacitance *C* (F g^{-1}), energy density E (Wh kg^{-1}),and power density P (W kg^{-1}) of the ASC were calculated by formulas 3, 4, and 5, where Δt (s) is the discharge time, *I* (A) is the discharge current, *m* (g) is the total loading mass of two electrodes,and ΔV (V) is the voltage window of the ASC.

$$C = \frac{I\Delta t}{\Delta m \Delta V} \tag{3}$$

$$\mathrm{E} = \frac{1}{2 \times 3.6} C V^2 \tag{4}$$

$$P = \frac{E \times 3600}{\Delta t} \qquad (5)$$

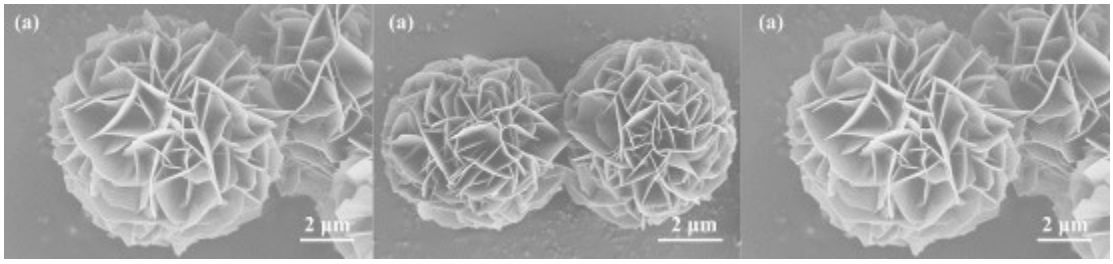

Figure S1. The morphology of (a) $Ni_2Co_1Al_1$-LDHs; (b) $Ni_{1.5}Co_{1.5}Al_1$-LDHs; and (c) $Ni_1Co_2Al_1$-LDHs in nanoflower structure.

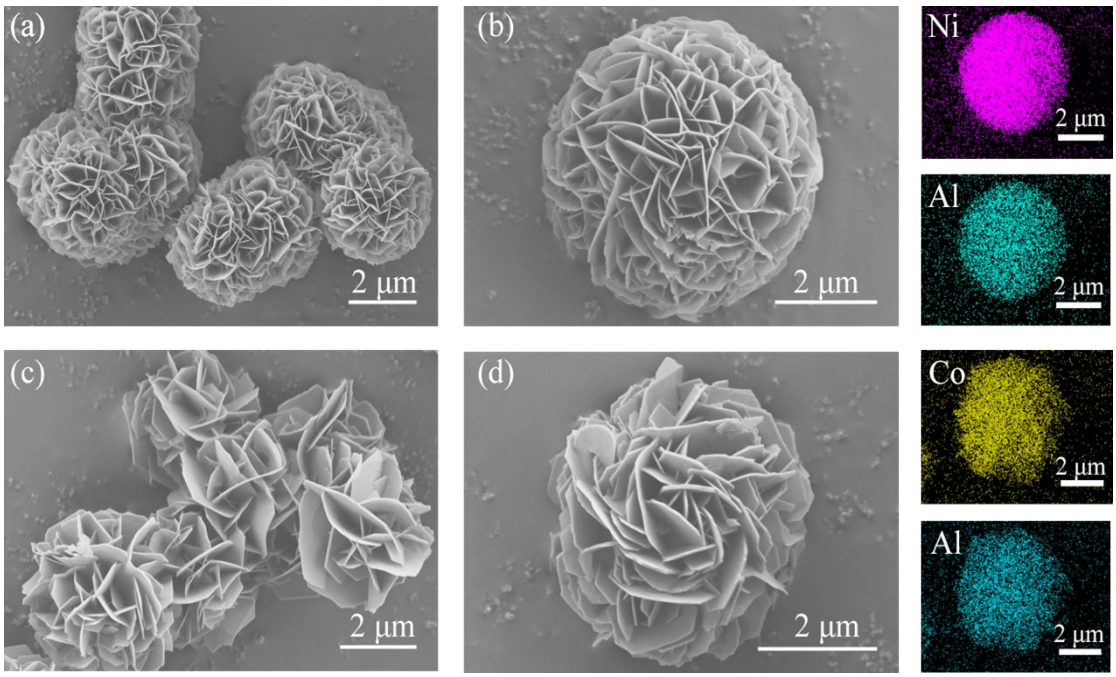

Figure S2. (a) overall and (b) single nanoflower structure of NiAl-LDHs and the corresponding elements mapping, (c) overall and (d) single nanoflower structure of CoAl-LDHs and the corresponding elements mapping.

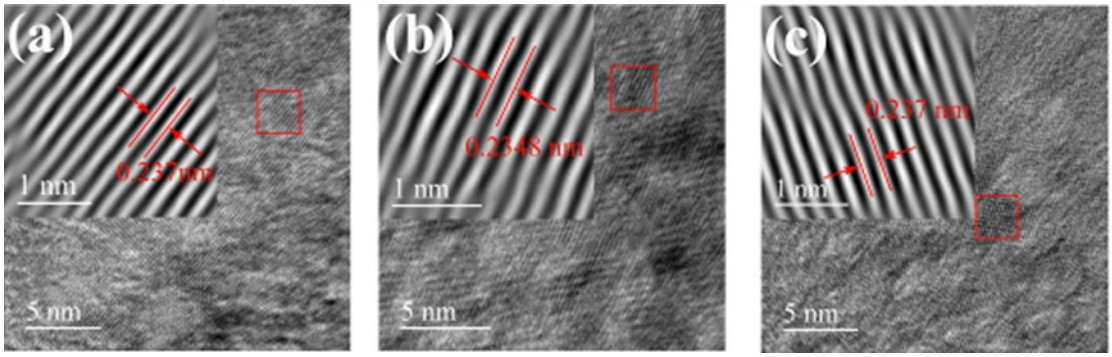

Figure S3. HRTEM of $Ni_2Co_1Al_1$-LDHs, $Ni_{1.5}Co_{1.5}Al_1$-LDHs and $Ni_1Co_2Al_1$-LDHs, the region selected for the FFT patterns inset in the upper left corner indicated by the red rectangle in (a), (b) and (c).

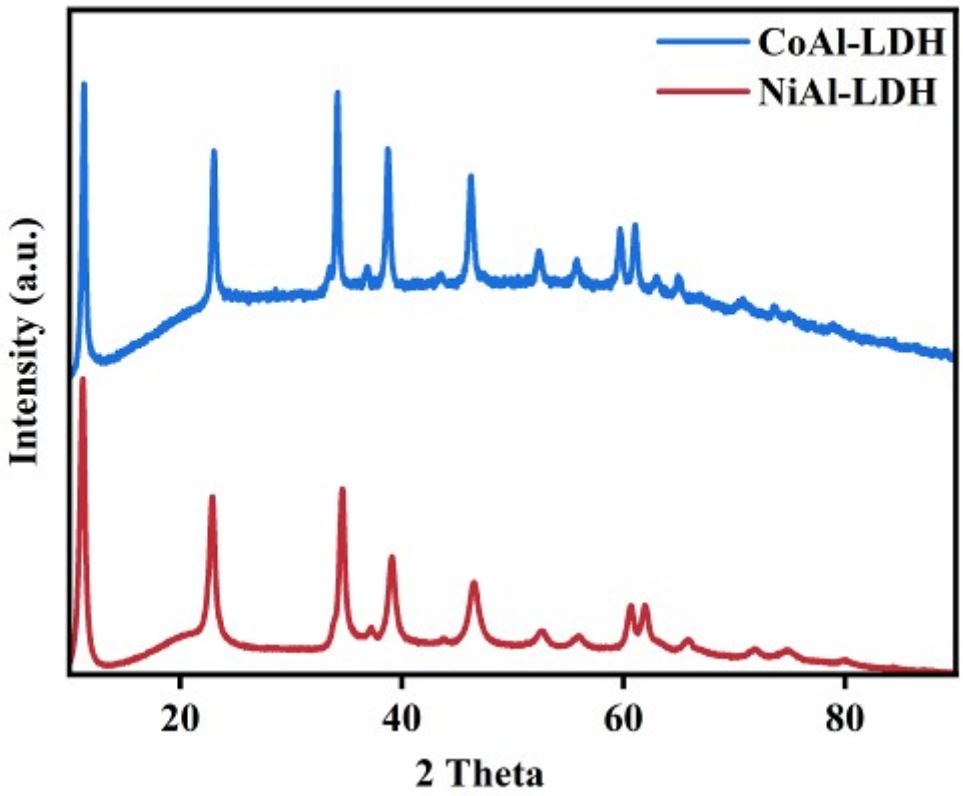

Figure S4. XRD patterns of CoAl-LDHs and NiAl-LDHs.

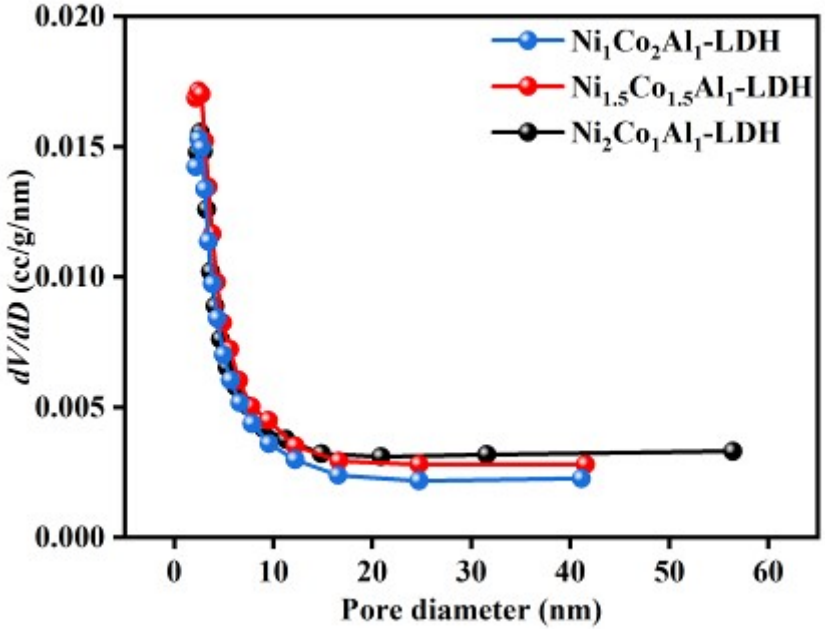

Figure S5. The pore size distributions of $Ni_2Co_1Al_1$-LDH,$Ni_{1.5}Co_{1.5}Al_1$-LDH and $Ni_1Co_2Al_1$-LDH,respectively.

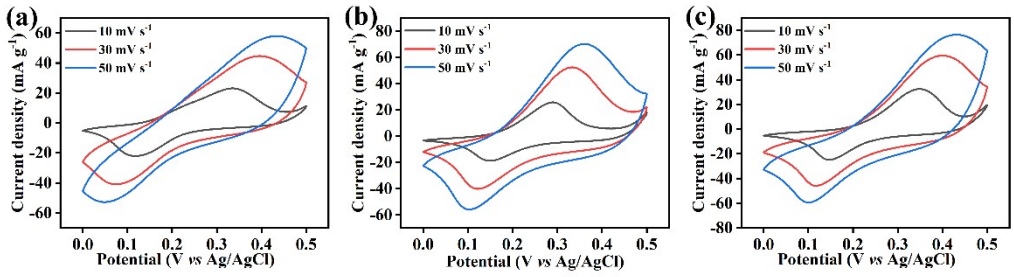

Figure S6. CV curves testing with scan rates increasing from 10 to 50 mV s^{-1} for (a) $Ni_2Co_1Al_1$-LDH; (b) $Ni_{1.5}Co_{1.5}Al_1$-LDH; (c) $Ni_1Co_2Al_1$-LDH electrodes.

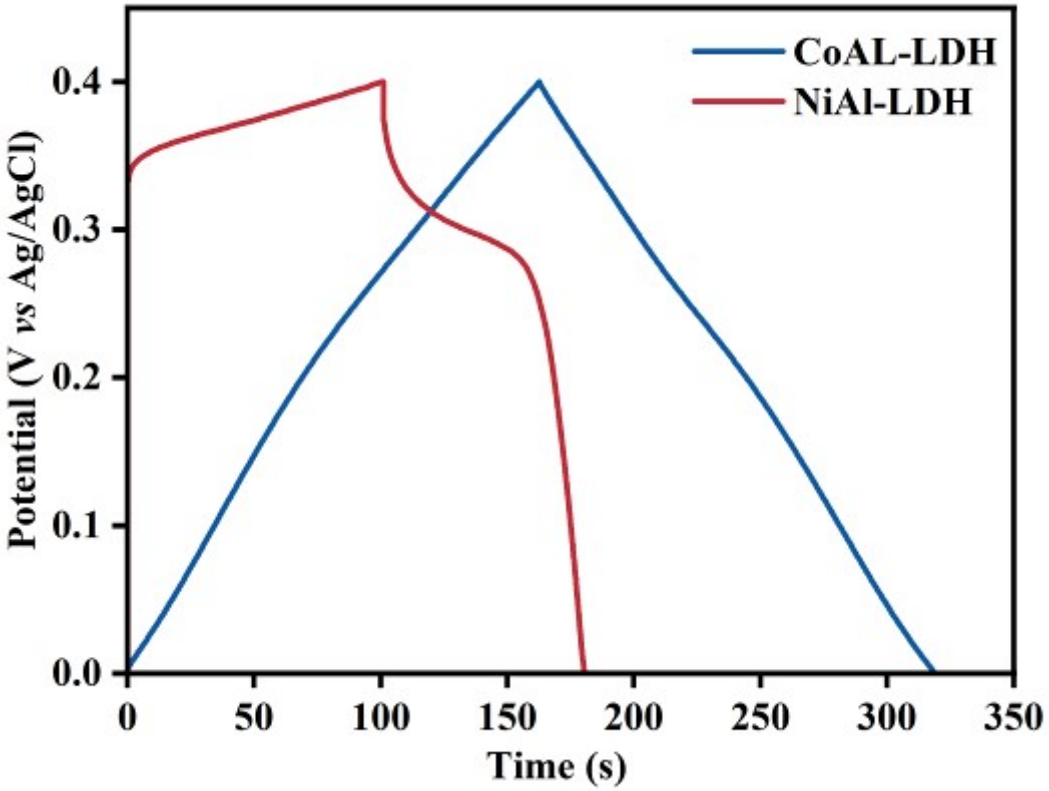

Figure S7. GCD curves of CoAl-LDHs and NiAl-LDHs with a testing current density at 1 A g^{-1}.

Table S1. Percentage of metal elements in all th e three samples.

Samples	Atomic (%)		
	Ni	Co	Al
$Ni_2Co_1Al_1$-LDH	13.45	6.79	6.0
$Ni_{1.5}Co_{1.5}Al_1$-LDH	7.56	9.81	5.79
$Ni_1Co_2Al_1$-LDH	6.08	12.98	6.29

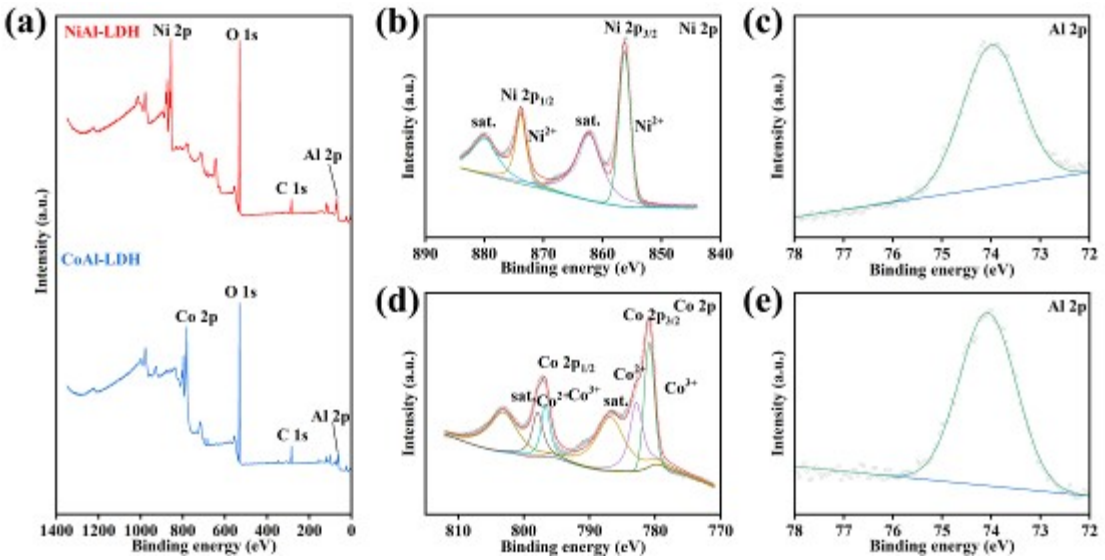

Figure S8. XPS spectra of (a) survey of NiAl-LDH and CoAl-LDH;(b) and (c) Ni 2p and Al 2p in NiAl-LDH;(d) and (e) Co 2p and Al 2p in CoAl-LDH.